ACS Sustainable Resource Management

pubs.acs.org/acssrm

Article

Evaluating the Scale-Up Potential of Biogenic Heterogeneous Catalyst for Biodiesel Production

Nabanita Ghosh, Rhithuparna D, Samuel Lalthazuala Rokhum, and Gopinath Halder*

Cite This: https://doi.org/10.1021/acssusresmgt.3c00111

Read Online

ACCESS | Metrics & More | Article Recommendations | Supporting Information

ABSTRACT: The increasing global population and its associated energy requirements significantly burden natural energy resources. The Paris Agreement's promises to prevent global warming and promote sustainable development are obscured by the fossil fuel industry's frightening rate of exploitation. Biodiesel offers a sustainable substitute for fossil fuels to solve viable fuel and socioeconomic issues. Diverse feedstocks, including *Jatropha* oil, palm oil, used frying oil, edible oil, animal fat, and microbial oil, are used to make biodiesel. Much exploration has been done on creating innovative and sustainable biodiesel synthesis technologies to boost the yield of biodiesel to remain competitive. In the current investigation, tamarind seed (*Tamarindus indica*) derived sulfonated doped carbon catalyst was utilized for the transformation of used cooking oil methyl ester (UCOME). The morphological and spectral analyses of the produced catalyst were performed thoroughly by means of TGA, BET, FTIR, XRD, and SEM-EDAX. The study of optimization of parameters that impact biodiesel efficacy was conducted using response surface methodology, which gave 98.97% conversion. The esterification reaction was examined by two kinetic models, and it followed the pseudo-first-order reaction kinetics with the reaction being endothermic and not spontaneous. The catalyst exhibited good reusability with 81.17% conversion until 4 cycles. The deactivation study of the prepared sulfonated catalyst (SDC) was analyzed. Additionally, fuel was ascertained by GC−MS, ^{1}H NMR, and FTIR evaluations. The anticipated cost of 1 kg catalyst and 1 L UCOME, as determined by cost analysis, were $3.706 and $0.403, respectively, demonstrating their excellent economic viabilities.

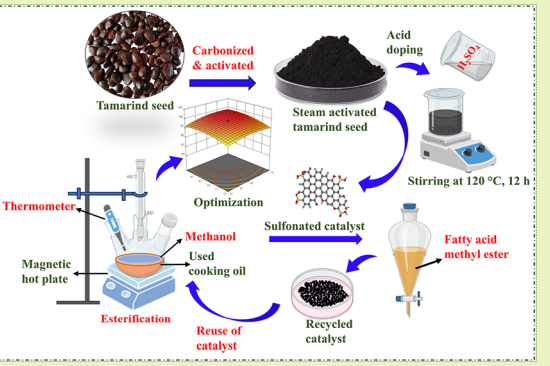

KEYWORDS: *Used cooking oil, Esterification, Tamarind seed, Response surface methodology, Life cycle cost analysis*

INTRODUCTION

Our energy sectors currently use fuels only made from fossil resources, which is raising concerns about the state of the world's oil reserves as well as the growing environmental effects of these fuels.[1] The enormous improvements in industrialization and motorization around the world have led to an increase in pollution levels that affect human health.[2] This goes hand in hand with the rise in energy demands given the scarcity of resources.[3] Therefore, alternative fuels that are made from renewable resources, address the energy and environmental crises, and burn cleaner than petro-fuels are required.[4] Biodiesel is regarded as one of the most suitable alternatives because of its renewability, structural and behavioral similarities to diesel, and lack of sulfur.[4] Furthermore, the number of pollutant discharges, viz., hydrocarbons, CO_2, and CO, from the engine is significantly reduced when using biodiesel or using it in combination with diesel.[5] To make biodiesel, a wide range of oil feedstock can be utilized. Soybean, peanut, coconut, corn, palm, and sunflower oils are utilized as edible oils, whereas inedible oils including neem, jojoba, apricot, cotton, and tobacco seed oils, lard, and used cooking oil (UCO) are also applied to make biodiesel.[6]

Commercializing biodiesel has been hampered mostly by manufacturing costs on a worldwide scale. It is generally agreed in the literature that the oily feedstock accounts for 80% or more of the entire production expenses.[7] Vegetable feedstock accounts for around 90−95% of the universal feedstock used in biodiesel manufacturing.[8] Moreover, the application of inedible oils requires additional pretreatment procedures. This leads to an understandable conflict between food and fuel, with the cost of edible oils rising as a result of their extensive use in the manufacture of fuel.[9] Conversely, inedible oils are prone to sporadic supply, but edible oils are widely available and provide a steady supply. UCO can be used to lower the biodiesel production costs because buying this oil does not incur additional expenses. Many people, especially in rural regions, dispose of used cooking oil directly into the environment

Received: November 23, 2023
Revised: February 24, 2024
Accepted: February 26, 2024

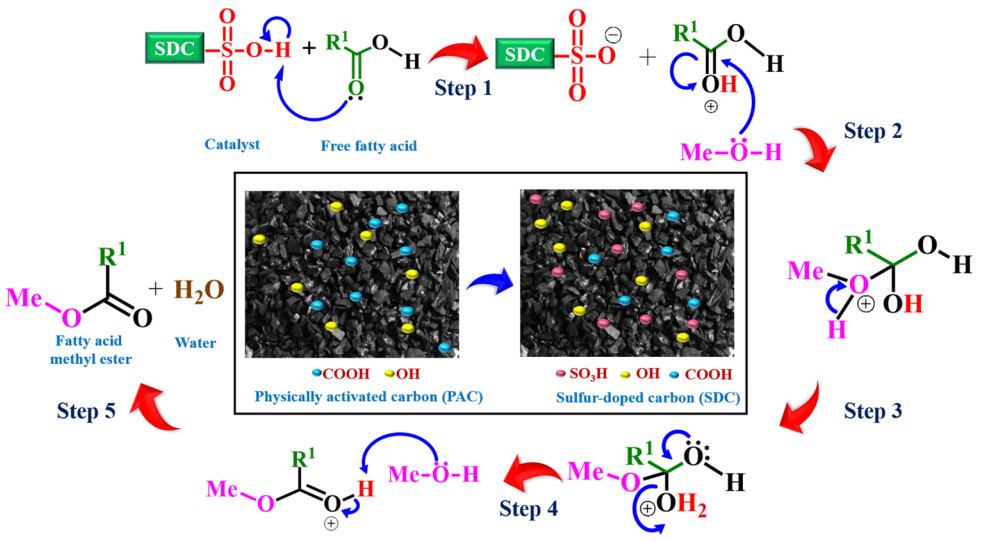

Figure 1. Esterification reaction mechanism of UCO to produce biodiesel.

because it is an expensive trash disposal option. To prevent pollution, these oils need to be treated before being discharged into the atmosphere.[10] Moreover, UCO minimizes conflict with food, as being an inedible oil. In addition to resolving one of the environmental issues that affect wastewater systems, this use can lower the costs of raw materials also.[11]

The most popular technique of biodiesel production is transesterification, which is a reversible reaction between oils and alcohol aided by a catalyst (even in industrial manufacturing).[12] Methanol is more widely utilized than ethanol because of its superior chemical characteristics and lower price. Catalysts used in these processes can be enzymatic, homogeneous, or heterogeneous.[13] Because of the high free fatty acids (FFA) level in UCO, it is suitable for biodiesel manufacture by esterification utilizing an acid catalyst. Hence, using a homogeneous base catalysis system to produce biodiesel from waste cooking oil presents serious problems for the final product's quality and purity. When soap and water are produced in the course of the saponification method, a high concentration of FFA in the feedstock can reduce the effectiveness of the alkaline catalyst.[14] H_2SO_4 and HCl are commonly used homogeneous acid catalysts although they are caustic and extremely corrosive.[15] As an alternative, high FFA oil can be produced as biodiesel in dual steps: first, it is esterified employing a homogeneous acid catalyst like H_2SO_4 and HCl and then it is transesterified using a base catalyst. However, the reactor is vulnerable to corrosion and has elevated manufacturing expenses because of the necessity of a further treatment step and the extremely concentrated acid catalyst.[16] The major difficulties related to homogeneous catalysts include problems of separation and purification of products, formation of soap, and overflowing wastewater owing to excessive washing of biodiesel, which hinders their application in biodiesel production. Since a solid catalyst can be effortlessly isolated from different phases and because it encourages a more ecologically friendly process, heterogeneous catalysis has been created to take the place of homogeneous ones.[17] A support to the catalyst is required to enlarge the surface area,[18] which improves catalyst stability while raising the reaction rate because remonstrance amid mass transfer redundancy lessens the rate of reaction.[19] Again, heterogeneous catalysis's diffusional resistances have an impact on the ultimate yield by slowing down the reaction rate.[20]

There have already been several reports of acid-functionalized heterogeneous catalysts in the direction of biodiesel manufacturing, viz., sulfonated synthetic coal, resin, 12-tungstophosphoric acid loaded bentonite clay, CM-SO_3H, HSO_3(Pmim), HSO_4, etc. The synthesis of these catalysts requires a number of steps and severe chemical conditions, which limits their practical use. These factors raise the overall cost of biodiesel production and decrease its environmental friendliness. However, producing biodiesel by the synthesis of catalysts made from waste biomass may offer a different, affordable, and sustainable method. Sulfonated carbonaceous catalysts are already utilized extensively in a variety of chemical processes, and it appears that this trend will continue.[21] Keera et al. were the first to introduce sulfonated carbonized organic material for the esterification of standard acid to convert into FAME.[22] Additionally, the activity of sulfonated carbon catalysts is on par with or even superior to those of the majority of traditional solid acid catalysts. Abdullah et al. prepared biodiesel employing waste cooking oil (WCO) using empty fruit bunch-based activated carbon with the biodiesel yield of 97.1%.[23] Gualberto Zavarize et al. reported an acid catalyst derived exploiting Amazon açaí berry seeds for producing biodiesel using spent cooking oil with 89% conversion.[24] Roslan et al. prepared biodiesel with 97% conversion from used cooking oil using sulfonated resin in 2 h reaction time.[25] A thorough review of the many works published in the last few years indicates that the use of biogenic precursor tamarind seeds for synthesizing carbonaceous char toward impregnation of catalyst has not been reported so far for esterifying used cooking oil to manufacture biodiesel (Figure 1 shows reaction mechanism).

In this study, a novel waste biomass, i.e., tamarind seed (*Tamarindus indica*), was employed to derive sulfonated catalyst (SDC) that was used as a reusable catalyst for the transformation of UCO to used cooking oil methyl ester (UCOME) over esterification. Utilizing UCO as feedstock further minimizes reliance on fossil fuels for energy production and indirectly lowers pollution. The primary objective of the research is to optimize the esterification reaction's critical parameters for escalated FFA conversion to UCOME, which

https://doi.org/10.1021/acssusresmgt.3c00111
ACS Sustainable Resour. Manage. XXXX, XXX, XXX−XXX

can be utilized as a replacement for traditional diesel. The effects of the optimized factor as time, temperature, acid catalyst weight, and methanol percentage were investigated. To maximize and improve the various interaction impacts of the aforementioned process parameters, the RSM-CCD technique is applied along with a conventional approach. Comparing the central composite design (CCD) to other optimization methods like the Box-Behnken and Doehlert matrix[26] reveals some significant advantages. Compared to other methods for optimizing, the CCD provides more experiments, which improves process optimization. The activation energy, the rate constant, and thermodynamic attributes were all examined through the use of kinetic research and thermodynamic analysis. After employing SDC catalysts, the UCOME is further examined and contrasted with ASTM requirements. A cost analysis of prepared UCOME and catalyst manufacture reveals that it is a comparably competitive technique with outstanding results. It is a tool made to quantify the environmental effects of production procedures, assisting in the making of decisions that support equitable development. Moreover, the deactivation mechanism of the synthesized SDC are critically discussed. Research on the catalytic effectiveness and failure mechanism of solid acid catalysts (SDC) is necessary to promote SDC for commercial usage.

RESOURCES AND TECHNIQUES

Resources. Methanol (99.50%), 2-propanol (≥99%), concentrated H_2SO_4 (98%), hexane (95%), KOH (≥85%), and phenolphthalein (pH indicator) were obtained from Merck India. For the synthesis of the sulfonated catalyst waste biomass tamarind seeds were accumulated from the regional areas of NIT, Durgapur campus. Used cooking oil was obtained from the nearby restaurants of Durgapur, West Bengal, India. The used cooking oil was heated and filtered to eradicate impurities. Without further purification, the chemicals were utilized. Deionized water was applied using an Arium-611 DI (Gottingen, Germany Sartorius A.G.) ultra-pure water system and used throughout the studies.

Synthesis of Catalyst. The conglomerated tamarind seeds were washed with water for stripping impurities following which seeds were dehumidified in an air oven; this sheds the moistness. About 100 g of seed was completely carbonized in a muffle furnace under a steady nitrogen atmosphere for 1.5 h at 500 °C. Ahead of the carbonization, the temperature of decomposition of the raw seeds was evaluated by thermogravimetric analysis (TGA) to figure out the temperature at which the loss of mass was reported as minimal and the residual mass remained constant. The carbonized seeds were physically activated for the advancement of surface qualities and accordingly, steam was supplied under 2−3 kg/cm^2 at 300 °C for 60 min.[27] The physically activated carbon (PAC) was then functionalized with concentrated H_2SO_4 following criterion approaches with some alterations.

In an archetypal technique, SO_3H groups were added into the PAC by loading 10 g of carbon with 100 mL of concentrated H_2SO_4 (1:8 w/v) at 120 °C for 12 h under 600 rpm agitation. After reaching out at normal temperature, the synthesized material was then washed frequently with water until sulfate ions (SO_4^{2-}) were no longer identified and filtered. The catalyst was then dehydrated at 80 °C in an oven for 8 h. The catalyst was designated sulfur-doped carbon (SDC). The SDC made was passed through a sieve of 0.2−0.5 mm to get a finer carbon catalyst.[1]

Catalyst Characterization. The highest temperature for carbonization of the tamarind seed is determined by TGA (Shimadzu, model C30574700290, Japan) synchronized with the DTA-TG apparatus. The temperature range for the TGA was 30−700 °C with 10 °C/min accretion and the flow rate was 19.8 mL/min for N_2 gas. An EDAX instrument (OXFORD INCAX- sight) was utilized to find inorganic elements. For determining the kind of a sample's structure through XRD analysis, an X-ray diffractometer (D8 ADVANCE BRUKER AXS made in Germany) is employed. Results were referred to the JSDPS standard library throughout a 10−50° 2θ range with 0.02 step size.[27] SEM (JEOL JSM-6030, India) examination was done to examine how the surface properties changed following the application of steam and H_2SO_4 impregnation. The inclusion of precise functional categories on the samples was determined using (FTIR C109292, spectrometer USA) FTIR. Using the Smart Sorb 92-93 (Smart Instruments, India) instrument, BET analysis estimates each sample's pore volume and surface area to determine its physical characteristics. The surface properties were calculated using the N_2 desorption−adsorption method while the working temperature was kept at 77 K.

Production of UCOME Using the Esterification Process. Used cooking oil was esterified in a 3-neck flat bottom flask accustomed with a magnetic stirrer hot plate which enables temperature modification so that the mixture temperature remains constant. A thermometer was installed on one neck to assess the mixture's temperature, and a condenser was installed on the other side of the flat bottom to lessen methanol loss by evaporation. Reagents were added over the middle neck. Methanol was added to the flask when the oil had been warmed to the necessary temperature. To ensure that the mixing was complete, the agitation was kept at 650 rpm. The catalyst was then introduced in the desired weight percentage. The duration of the reaction was determined by the prepared design matrix. When the reaction was ended, the catalyst was recovered by utilizing Whatman 1 filter paper and was repeatedly cleaned with hexane to shed the oil. Using a rotary evaporator, excess methanol was collected from the reaction mixture. After that, the mixture is placed into a separating funnel and kept for the entire next day so that it can separate into noticeable layers. The bottom layer is an aqueous phase that contains water that has been drained, while the top layer contains used cooking oil methyl ester (UCOME). To measure the decrease in FFA% of the sample, titration was performed with 0.01 N KOH.[28]

Design of Experiments (DOE) via CCD Approaches. The approach of using one factor/parameter at a time (OFAT) is not suitable for the effective optimization of parameters since numerous conjoining tests are needed to complete the process, which substantially decreases the cost and time of optimization. To find the lesser number of meaningful runs between related attributes at multiple levels of each attribute which are acceptable to estimate the ideal reflex within a lowered number of exploratory runs, a software-guided approach like response surface methodology (RSM) is preferred. For the esterification of UCO for UCOME synthesis, the influencing parameters of the process are catalyst loading, methanol concentration, reaction temperature, and time. In this research work, 4 parameters are considered for the CCD matrix. Using eq 1, N can be represented below as

$$N = A + C + F = 2^n + 2(n) + n_c \quad (1)$$

https://doi.org/10.1021/acssusresmgt.3c00111
ACS Sustainable Resour. Manage. XXXX, XXX, XXX−XXX

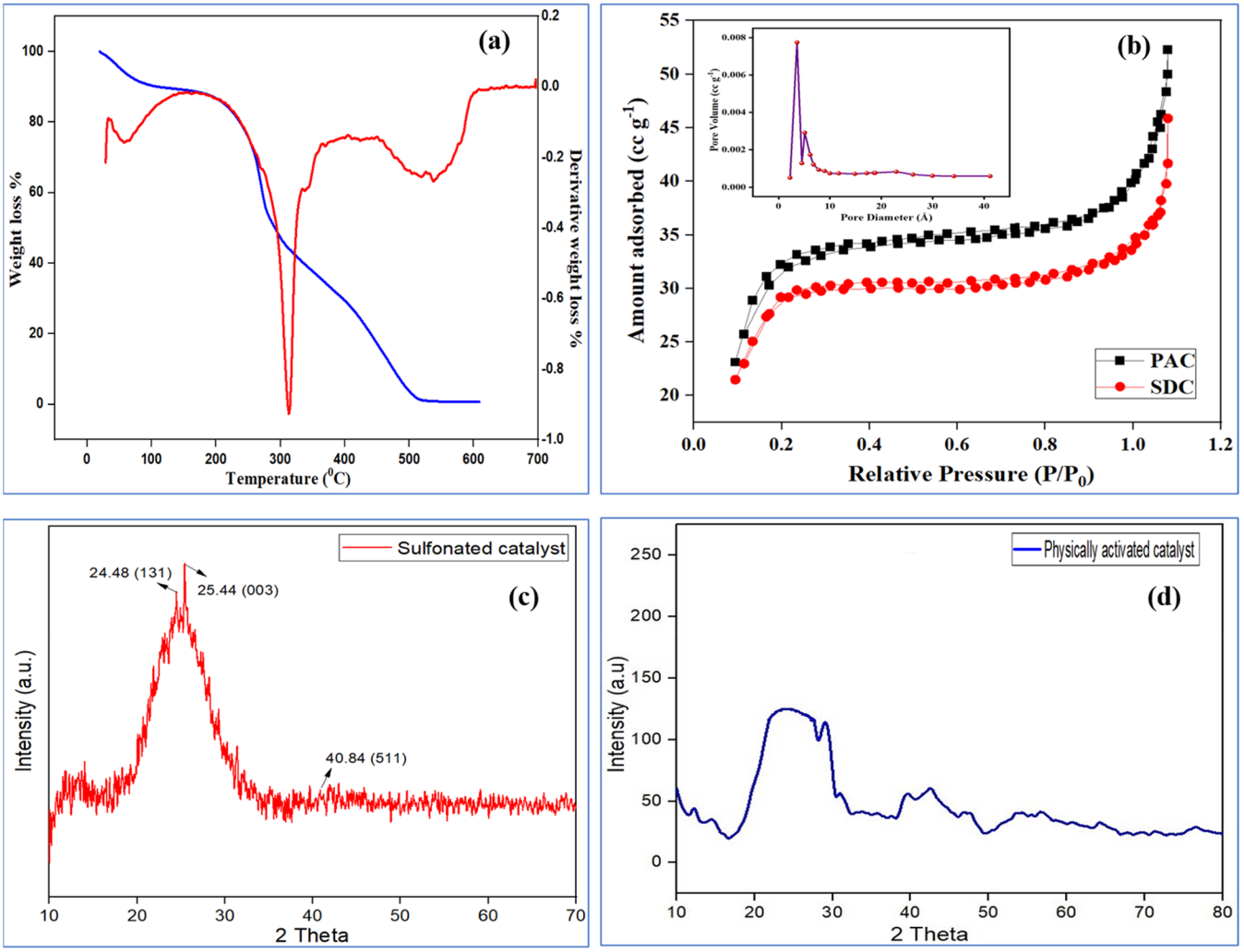

Figure 2. TGA and DTGA graph (a), N_2 adsorption−desorption isotherm and BJH pore size distribution curve (b), and XRD patterns of sulfonated catalyst (SDC) (c) and physically activated catalyst (d).

N = the summation of all the runs, $A = 2^n = 8$ = axial runs, $C = n_c = 6$ = center runs, and $F = 2(n) = 16$ = factorial runs.

This statistical study is covered by fit and comparability of models' statistics, as well as analysis of variance (ANOVA). The different variables along with their parametric level used for the optimization study are listed in Table 4. Parametric contribution is attained using eq 2:

$$\text{Contribution factor } (\%) = \left(\frac{SS_f}{SS_T}\right) \times 100 \quad (2)$$

where SS_f = sum of squares of a particular factor and SS_T = sum of squares of the model.

RESULTS AND ANALYSIS

Characterization of the Synthesized Carbon Catalyst. The thermal strength of the prepared (SDC) catalyst was evaluated by thermogravimetric analysis, as shown in Figure 2(a). There are two main peaks in thermal deterioration; one is below 100 °C and is attributed to water loss. The other peak, which occurs from losses of volatile organic components (VOC), is between 200 and 400 °C. Since no mass loss is observed beyond 500 °C, it is inferred that the remaining mass is solely carbonaceous in origin. For this reason, 500 °C is chosen as the carbonization temperature.

The surface area (SA) and pore volume (PV) of PAC and SDC were calculated from BET analysis as displayed in Figure 2(b), which depicted: (a) surface area of the carbon has improved by physical activation through steam owing to the formation of micropore on the surface of the PAC and (b) H_2SO_4 impregnation has blocked the micropores of PAC and resulted in the formation of SDC. PAC has a PV of 0.264 cm^3/g and SA of 807.4 m^2/g while the PV and SA for SDC are 0.0715 cm^3/g and 329.53 m^2/g subsequently. The produced SDC catalyst exhibits a shift in surface area and a matching drop in PV, suggesting that H_2SO_4 did indeed successfully dope the PAC support.

The crystalline structure of the prepared SDC and PAC can be understood utilizing the XRD analysis results, which is seen in Figure 2c,d. To identify the diffraction peaks, a typical JCPDS library is used. The peaks obtained within the range 20°−30° at 2θ values of 24.48° and 25.44° validate that the nature of the support is carbonaceous. The diffraction pattern for SDC is observed to form an elevated peak between 20° and 30° and an additional mini peak between 41° and 49°. The observed peak at the planes (131, 003, and 511, respectively) provides evidence of successful H_2SO_4 doping of the carbon

https://doi.org/10.1021/acssusresmgt.3c00111
ACS Sustainable Resour. Manage. XXXX, XXX, XXX−XXX

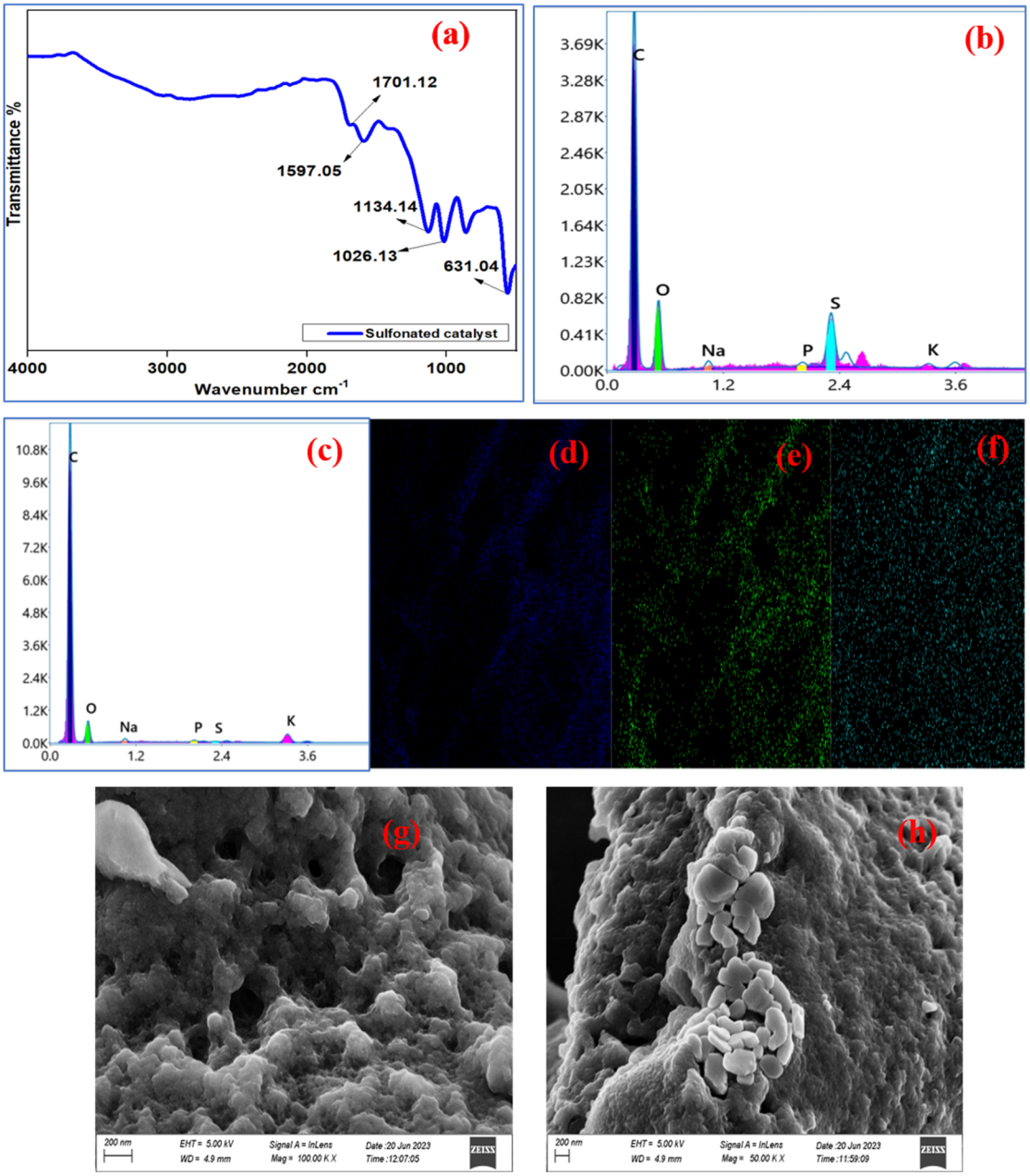

Figure 3. FTIR graph of sulfonated catalyst (a), EDAX analysis of PAC (b), SDC (c) along with elemental mapping of carbon (d), oxygen (e), and sulfur (f), SEM images of physically activated carbon (PAC) (g) and sulfonated catalyst (SDC) (h).

support on the PAC catalyst, further supported by FTIR analysis.

The FTIR graph is displayed in Figure 3a for SDC catalysts. The following are the peaks that are present at various characteristic wavenumbers: 1026.13 and 1134.14 cm^{-1} signify sulfur as sulfoxide and sulfone (S═O).[29] 1597.05 cm^{-1} indicates C═C alkene bond, and 1701.12 cm^{-1} refers to C═O bond of the carbonyl group. Moreover, the transmission peak at 631.04 cm^{-1} represents the sulfur group ($-SO_3H$) and validates successful H_2SO_4 adsorption on the SDC catalyst. The SDC ascertained the occurrence of numerous and necessary components on the matrix upon EDAX analysis, indicating doping in Figure 3b−f). This coincides with a sharp peak for S and O in SDC Figure 3b. The doping of sulfur on the physically activated carbon can be additionally validated by the SEM pictures. As a result of the steam flow, Figure 3g demonstrates that the produced PAC support has many pores that can adsorb sulfur groups. This indicates that the carbon's surface characteristics were perfectly altered by the superheated steam utilized during the activation procedure, which created pores. Further, Figure 3(h) substantiates the revelatory adsorption of H_2SO_4 in the surface and the pores, resulting in surface smoothing and pore blockage in the SDC catalyst.

The XPS measurement performed on the SDC catalyst is depicted in Figure 4, which confirms the existence of C, O, and S on the catalyst surface. The bending energies of 292.15 eV (C═O) and 284.14 eV (C═C) correspond to the C 1s shown in Figure 4a. The peak at 533.56 eV corresponds to the O 1s spectra as shown in Figure 4b.[30] Moreover, XPS analysis shows the $-SO_3H$ group. The single peak obtained at 172 eV indicates the $-SO_3H$ group concerning to S 2p as depicted in Figure 4c.[31]

https://doi.org/10.1021/acssusresmgt.3c00111
ACS Sustainable Resour. Manage. XXXX, XXX, XXX−XXX

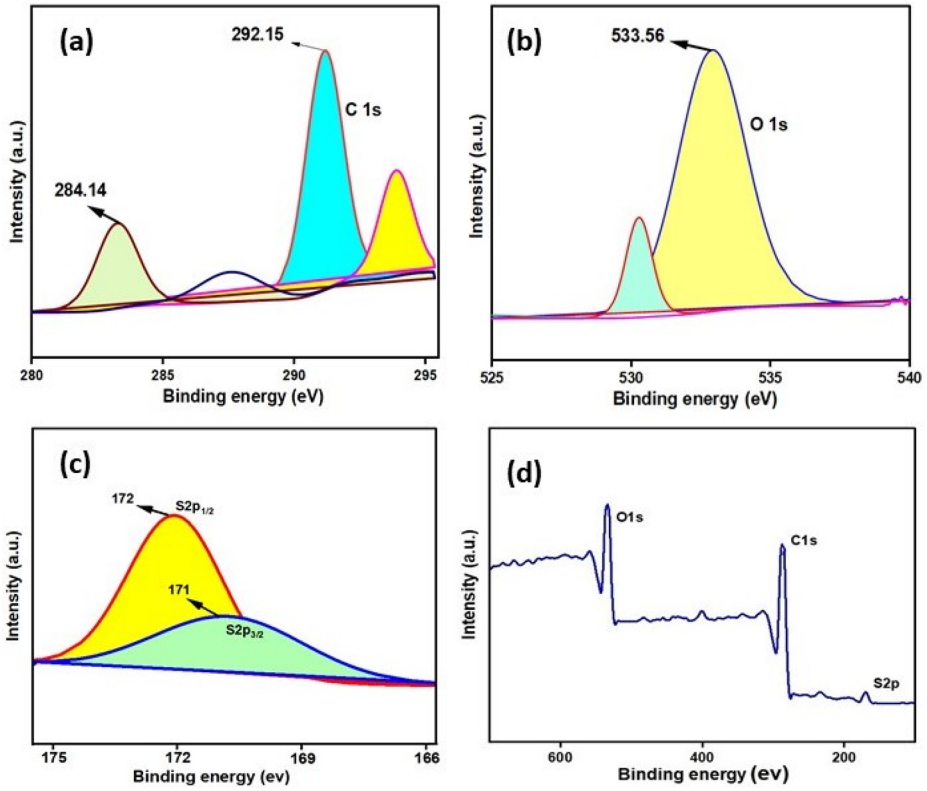

Figure 4. XPS analysis of SDC catalyst. Experimental spectra for C 1s (a), O 1s (b), and S 2p (c) regions and XPS survey spectrum of SDC (d).

Table 1. RSM (CCD) Matrix Utilized in the Used Cooking Oil Conversion

Run	Catalyst conc wt % (*A*)	Methanol conc wt % (*B*)	Time (min) (*C*)	Temperature (°C) (*D*)	Actual FFA conversion (%)	Predicted FFA conversion
1	5	40	90	60	98.59	98.79
2	4	50	120	65	98.71	98.86
3	6	30	60	65	86.38	86.50
4	3	40	90	60	86.89	86.98
5	5	40	90	60	98.97	98.73
6	4	30	60	65	90.57	90.79
7	4	50	60	65	96.88	96.63
8	4	30	120	65	95.47	95.60
9	5	40	150	60	97.42	97.31
10	5	40	90	60	98.54	98.73
11	6	30	120	65	91.37	91.25
12	7	40	90	60	85.98	85.84
13	6	50	120	65	90.73	90.95
14	5	20	90	60	91.59	91.44
15	5	40	90	60	98.82	98.73
16	6	30	120	55	97.34	97.53
17	5	60	90	60	95.31	95.58
18	6	50	60	55	88.39	88.20
19	6	50	120	55	95.62	95.58
20	4	30	60	55	80.99	81.71
21	4	50	120	55	92.54	92.36
22	5	40	90	60	98.78	98.73
23	6	50	60	65	88.71	88.84
24	4	30	120	55	90.74	90.80
25	5	40	90	50	90.45	90.54
26	5	40	90	70	96.19	95.98
27	5	40	30	60	85.13	85.12
28	5	40	90	60	98.67	98.73
29	4	50	60	55	84.61	84.99
30	6	30	60	55	87.403	87.59

https://doi.org/10.1021/acssusresmgt.3c00111
ACS Sustainable Resour. Manage. XXXX, XXX, XXX−XXX

Modeling and Statistical Analysis of UCOME Using RSM. The esterification reaction was optimized using experimental matrix RSM under central composite design (CCD).[32] UCOME conversion varied from 80.99 to 98.97%, per testing run. The actual and anticipated results for individual experimental runs are shown in Table 1. As shown in eq 3, the coded factors A through D have an impact on the UCOME conversion.

$$\begin{aligned}\text{FFA Conversion} = {} & 98.73 - 0.2661A + 0.9736B + 3.05C \\ & + 1.36D - 0.8758AB - 0.0416AC \\ & - 2.77AD - 0.6604BC + 0.4096BD \\ & - 1.32CD - 3.09A^2 - 1.33B^2 \\ & - 1.88C^2 - 1.37D^2 \end{aligned} \quad (3)$$

where A = catalyst weight, B = concentration of methanol, C = reaction duration, and D = temperature, respectively. The "+" indication signifies that a parameter in the regression equation has a positive influence on the reaction process, considering the "−" sign signifies a negative impact on the reaction as a result of the selected parameter.

The results of the investigative runs are assessed and consolidated utilizing ANOVA statistical analyses as seen in Table S1. The model's F-value was high enough to demonstrate the model's relevance. Additionally, a p-value below 0.0001 indicates the numbers in the advocated model were revealed by accident, additionally demonstrating the reliability of the outcomes. Additionally, the model shows a significant correlation between actual and hypothetical data, with the R^2 values for hypothetical and actual data as shown in Table S2 (0.9954 and 0.9982, respectively) differing by less than 0.2. The model's appropriate precision (AP) value, which must be at least 4, is substantially higher at 114.4298 than it is at 4. High AP values suggest accurate, error-free outcomes from the trial. As stated in Table S3, the effect of important parameters can be listed as follows: catalyst loading = 5.48%, methanol weight = 0.21%, reaction time = 27.49%, and temperature = 2.80%.

Diagnostic graphs are utilized to predict the reliability of the regression line (Figure S1). The projected and actual UCO conversion to UCOME is contrasted in Figure S1a. The residuals, or the discrepancies between actual and anticipated values, are used to gauge the suitability of the ANOVA model with the assumptions. A comparability of the experimental run and the expected is shown in Figure S1b. A considerable residual difference between runs was noticed because of experiment noise. The fitted model records no mistakes because all residuals are within the range of 4.00. The comparison of the actual and anticipated conversion of UCOME is shown in Figure S1c. The propinquity of the numbers to the regression line indicates a decent estimate of the result for variations in the individual attributes. A normal distribution must be assessed in terms of the residuals for it to be regarded as genuine. Figure S1d shows the relationship amid a normal distribution and the studentized residuals where the data follow linear trends.

Influence of Factors on Used Cooking Oil Conversion to UCOME. A three-dimensional diagram Figure S2 was applied to assess the outcome of autonomous parameters on the synthesis of UCOME from used cooking oil. The resemblance between MeOH content and temperature is seen in Figure S2a. The plot clearly shows that the FFA conversion increased as temperatures and MeOH% increased. The UCOME conversion was 98.97% when the MeOH content was 40% w/w at 60 °C. Over a 40 wt % methanol concentration, the conversion drastically reduced. That can be confirmed as methanol is employed in large quantities to dilute the reaction mixture and add water.

The impact of catalyst A% and time over FFA transformation is displayed in Figure S2b. Owing to the existence of additional active components as the catalyst dosage was elevated, the conversion significantly increased.[32] However, despite repeated enhancement in catalyst, the utmost FFA conversion was observed. The esterification reaction is reversible; therefore, the highest conversion was seen at 90 min and decreased after that.

Temperature and reaction time are ascertained to influence the feedstock conversion as shown in Figure S2c. After 90 min at 60 °C, conversion was 98.97%. The 3D figure shows how the two factors strongly interact. Figure S2d portrays the interacting impact of the amount of the catalyst and methanol on the transformation of UCOME. The conversion elevated as the catalyst and MeOH concentrations increased, reaching their maximum point, respectively. Following esterification is reversible in nature when the reaction is prolonged past the optimal value, a mild decline in conversion can be seen. When MeOH is introduced in excess, the system becomes diluted, which has an impact on the reactions and conversion rates of the reactants. However, a small concentration of MeOH is inadequate to halt a retrograde reaction. In this study, the catalyst concentration was kept at 3 to 7% w/w, with 5 wt % depicting the utmost transformation. Because they are heterogeneous, catalysts in excess can cause diffusional defiance between alcohol and UCO.

The relationship between reaction time and MeOH concentrations is depicted in Figure S2e. At low methanol concentrations, conversion efficiency did not increase while the reaction time was enhanced from 60 to 120 min. The maximum UCOME conversion was at 40% MeOH concentration after 90 min, despite large variability; changing the period had little effect on the result. The resemblance amongst catalyst weight and temperature is depicted in Figure S2f. The ideal temperature for conversion was 60 °C. Since esterification is an endothermic reaction, conversion was initially improved by raising the temperature.

Kinetic and Thermodynamic Analysis of Esterification. To identify the kinetic order of the heterogeneous acid esterification method, the reaction was considered to be pseudo-homogeneous. The concentration of FFA decreases as the process progresses. Because esterification reactions are reversible in nature, an extra volume of methanol must be given to shift the reaction in a positive direction. Considering that, the rate of the reaction can be written as

$$-\left(\frac{dC_{ffa}}{dt}\right) = kC_{ffa}^{n} \quad (4)$$

$$C_{ffa} = C_{ffa_0}(1 - x) \quad (5)$$

where k, c_{ffa}, c_{ffa_0}, and X indicate reaction rate constant, the concentration of FFA, primary FFA concentration, and fractional ester conversion, respectively. Moreover, eq 5 can be rewritten as eq 7.

https://doi.org/10.1021/acssusresmgt.3c00111
ACS Sustainable Resour. Manage. XXXX, XXX, XXX−XXX

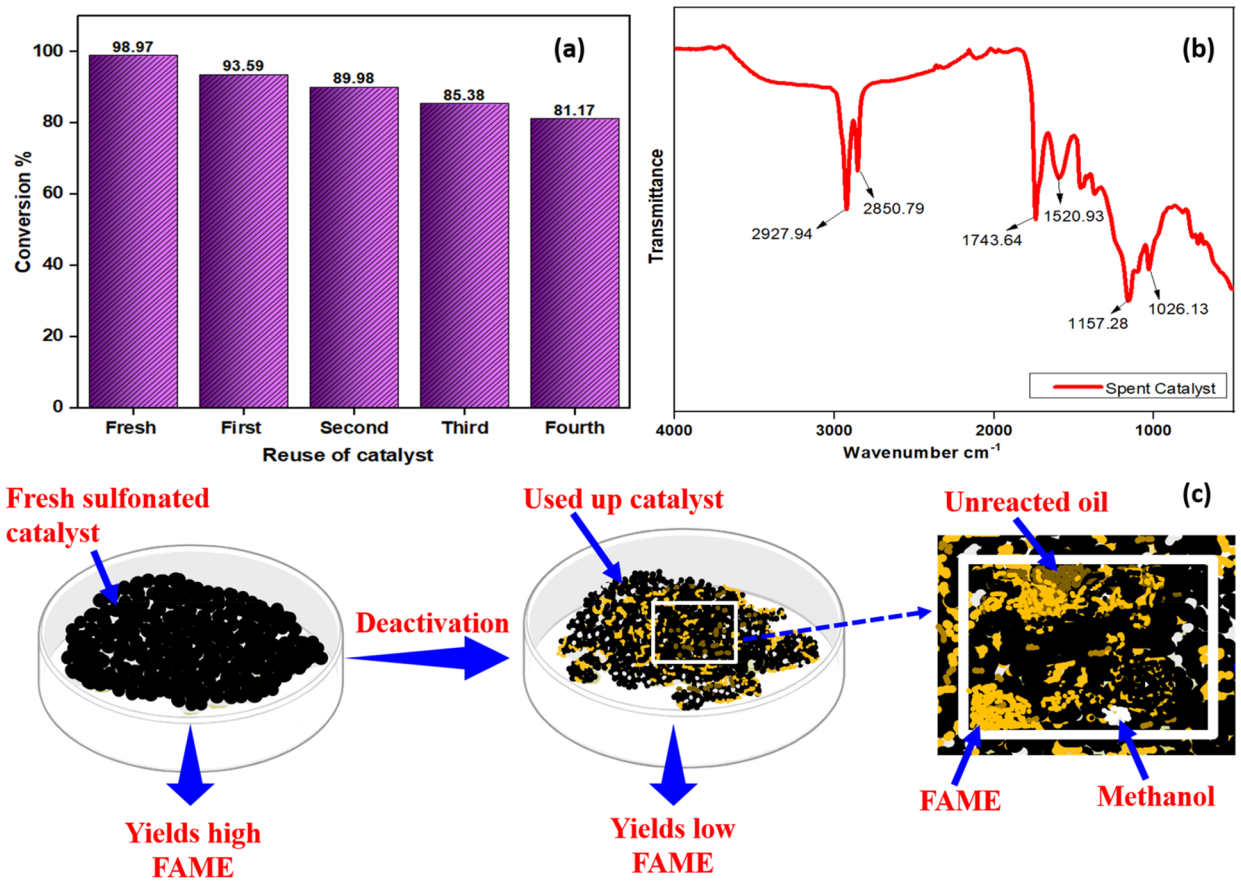

Figure 5. (a) Reusability of SDC catalyst for esterification reaction. Experimental conditions: methanol weight, 40 wt %; catalyst weight, 5 wt %; temperature, 60 °C; time, 90 min. (b) FTIR spectra of reused catalyst (after 4 cycles). (c) Scheme for catalyst deactivation process.

$$-\left(\frac{dx}{dt}\right) = \left(\frac{k}{C_{ffa_0}}\right)[C_{ffa_0}(1-X)]^n = K_1[C_{ffa_0}(1-X)]^n \quad (6)$$

$$\ln(1-X) = -kt \quad (7)$$

$$\frac{X}{(1-X)} = kC_{ffa_0}t \quad (8)$$

For $n = 1$ (first order) and for $n = 2$ (second order), eq 6 can be shown as eqs 7 and 8 subsequently. The influence of the increasing temperature on UCOME transformation was assessed by varying the temperature from highest to lowest selected in the CCD matrix. The optimization research led to the selection of the temperature range for the kinetics investigation. Figure S3a,c shows linear correlations between time vs $-\ln(1-X)$ and $X(1-X)$ for reaction temperatures ranging between 45 and 60 °C. The graphs in Figure S3b,d depict pseudo-first-order and second-order kinetics. When the linear regression coefficients (R_2) were compared, it was discovered that the pseudo-first-order model reported a higher R_2 (0.9841) compared to the R_2 (0.9696) for the second order.[33] This supports our hypothesis that esterification occurs as an outcome of pseudo-first-order kinetics. To estimate the activation energy (E_a) and k value of the esterification reaction Arrhenius equation was employed, as represented in eq 9,

$$\ln k = -\frac{E_a}{RT} + \ln A \quad (9)$$

where E_a = activation energy, R = universal gas constant, A = Arrhenius constant, T = temperature (K), and X = UCO conversion to UCOME. The graph between $\ln k$ and $1/T$, as shown in Figure S3b gives the energy of activation is 61.012 kJ mol^{-1} for the pseudo-first-order reaction kinetic model. This E_a value is in the range 25.8−83.2 kJ mol^{-1} usual for trans/esterification as reported by other studies.[34,35] Besides, intercept and slope values obtained from Figure S3e are used to calculate the thermodynamic parameters, viz., enthalpy (H^0) and entropy (S^0). The Eyring−Polanyi equation illustrates how thermodynamic parameters are connected, as demonstrated in eq 10,

$$\ln\frac{k}{T} = \frac{\Delta S^0}{R} - \frac{\Delta H^0}{RT} + \ln\left(\frac{k_b}{h}\right) \quad (10)$$

where h and k_b signify Planck's and Boltzmann's constants, respectively. The values of enthalpy and entropy were ascertained to be 58.306 kJ mol^{-1} and −0.0911 kJ K^{-1} mol^{-1}, correspondingly. The related ΔG^0 value is produced by replacing the results of (H^0) and (S^0) in eq 11,

$$\Delta G^0 = \Delta H^0 - T\Delta S^0 \quad (11)$$

If H^0 is positive, the reaction is endothermic; if S^0 is negative, the process is less chaotic. The positive ΔG^0 value of 88.66 kJ mol^{-1} at 60 °C indicated that the reaction was not spontaneous at any temperature.

Stability Test and Deactivation Study. The catalysts were easily recovered by filtration after the initial cycle, cleaned with hexane, and heated at 120 °C. After the first recycling

https://doi.org/10.1021/acssusresmgt.3c00111
ACS Sustainable Resour. Manage. XXXX, XXX, XXX−XXX

Table 2. Cost Analysis of Catalyst Synthesis

Stage	Details	Price ($)
Cost of waste biomass (CWB)	Waste biomass is locally available.	$0
Cost of biomass washing (CBW) = EC (electricity cost) + WC (washing cost)	EC = units required × unit price for water = 1 × $0.037 WC = $0	$0.037
Drying cost of waste biomass (DRWB)	Time (h) × units required × per unit cost = 10 × 1.5 × $0.037	$0.56
Cost of carbonization (CC) = IEC (IEC = inert gas costs) + EC (electricity cost)	IEC = N_2 flow = $0.031 EC = Time (h) × units required × per unit cost = 1.5× 5× $0.037=$0.278 CC= $0.031 + $0.278	$0.309
Physical activation cost (PAC) = SC (steam preparation cost) + EC (electricity cost)	SC = Time (h) × units required × per unit cost = 1 × 1 × $0.037 = $0.037 EC = Time (h) × units required × per unit cost = 1 × 3 × $0.037 = $0.111PAC = $0.037 + $0.111	$0.148
Biomass preparation cost (BPC)	CWB + CBW + DRWB + CC + PC = $0 + $0.037 + $0.56 + $0.309 + $0.148	$1.054
Doping cost (DC) = RC (rotation costs) + PCCH (pure cost of chemicals)	RC = Time (h) × units required × per unit cost = (12 × 0.5 × $0.037) = $0.222 CCH = [amount of H_2SO_4 required (L) × per litre cost] = 4 × $3.05 = $12.2 DC = $0.222 + $12.2	$12.422
Net cost of catalyst (NCC)	Biomass preparation cost (BPC) + Doping cost DC = $1.054 + $13.76	$13.476
Total cost of catalyst/kg	= NCC + extra cost (10% of $ 13.476) = $13.476 + $1.3476	$14.824
Total cost of catalyst (1 kg) after four cycle	= catalyst synthesis cost/no. of cycles for use = $14.824/4	$3.706

trial, the yield of FAME decreased marginally to 93.59% and remained largely consistent up to the fourth recycling experiment. The catalyst was frequently exploited in additional catalytic reactions with varying catalyst loading under preset conditions to evaluate its efficacy. The catalyst had good catalytic activity for the first four cycles as shown in Figure 5a. However, in our research, we found that the sulfonated carbon catalysts' activity decreased with each recycling cycle, and a sharp decline was seen after the fifth recycling trial. The two main causes of deactivation were methylation of $-SO_3H$ and leaching of active phases. UCOME and unreacted UCO were found in the spent catalysts during FTIR analysis, which suggests that it may have contributed to the catalysts' deactivation. From Figure 5b the peak observed at 2927.94 and 2850.79 cm^{-1} corresponds to the CH_2 and CH_3 group, confirming the presence of ester and feedstock. The transmission peaks at 1743.64 and 1520.93 cm^{-1} signify C═O and C═C stretching vibrations, which validate the occurrence of more esters on the catalyst surface. After each cycle, the unreacted oil and ester remained on the catalysts' surfaces, preventing the resulting mixture from diffusing into the $(-SO_3H)$ groups' active centers Figure 5c.

Cost Analysis of Catalyst and UCOME. The cost analysis can be utilized as an approach to measure the progress of biodiesel production. The price of the feedstock and other expenditures make up the cost analysis. By considering all the factors, involving the origin of the waste biomass, the synthesis process, the applied treatment procedure, and especially reusability, the cost evaluation for the synthesis of catalysts for the current work is evaluated to establish whether the strategy is viable. An essential technique that can reveal the production chain's more efficient operations and point the way toward improving biodiesel production is the systematic examination of mass and energy equations at each stage of the process. Given that we spent $1.054 preparing the waste-derived activated carbon, which is less compared to commercially available activated carbon, i.e., $14.5, making the current approach profitable for commercialization. Therefore, since the cost of raw materials is essentially nonexistent, using waste precursors gives a clear advantage. For the present work, the costs for SDC without reuse are around $14.824; nevertheless, after 4 reuses, the costs are only $3.706. All prices were displayed in US dollars ($) and were based on the detailed synthesis as shown in Table 2. In contrast, the cost of feedstock is also nil since used cooking oil is obtained free of cost from a local vendor. The approximate production cost of 1 L UCOME using an SDC catalyst is $0.403 as shown in Table 3.

Table 3. Cost Analysis of Used Cooking Oil Methyl Ester

Step	Description	Amount
Cost of Used cooking oil for 100 L UCOME production	Used cooking oil is freely available.	$0
Catalyst used for UCOME (100 L)	4.075 kg	$15.102
Price of methanol required for UCOME	(Quantity × cost of methanol/kg) (45 × $0.40)	$18
UCOME preparation cost (experimental time (h) × units × cost)	(1.5 h × 40 × $0.037)	$2.22
Additional expenses	(Washing cost + miscellaneous)	$1.80
Net cost of UCOME (100 L)	($0 + $15.102 + $18 + $2.22 + $1.80)	$37.122
Extra cost	10% of $37.122	$3.7122
Absolute cost of UCOME (100 L)	$37.122 + $3.7122	$40.2942
Absolute cost of UCOME (1 L)	$40.2942 ÷ 100	$0.403

Comparability of the Synthesized Catalyst with Other Sulfonated Catalysts. Several waste biomass-based heterogeneous catalysts were used for biodiesel production using waste cooking oil, according to the literature. Sulfonated carbonated coconut meal residue,[36] sulfated Ce supported activated carbon obtained from coconut shell,[37] etc., showed high conversion of WCO oil, but they require very high temperatures. Table 4 summarizes the relevant facts for comparison with our created catalyst, such as operating parameters, catalyst type, reaction temperature, and time. Through the literature review, it can be outlined that the preceding work has severe flaws. Long reaction times can be seen in refs 38 and 39 to produce biodiesel, as well as a high molar ratio.[40,41] However, several heterogeneous catalysts, such as palm kernel shell,[42] rubber de-oiled cake,[43] cacao shell,[44] etc., can be made from waste biomass, curbing the inclusive cost of biodiesel manufacturing. Nevertheless, the

https://doi.org/10.1021/acssusresmgt.3c00111
ACS Sustainable Resour. Manage. XXXX, XXX, XXX−XXX

Table 4. Comparability of the Synthesized SDC with Formerly Reported Acidic Catalyst

Catalyst	Feedstock	Parameters[a]	Conversion/yield (%)	Reference
Coconut meal residue	Waste palm cooking oil	12:1, 5, 150, 180	95.5	36
Coconut meal residue	Waste palm oil	12:1, 5, 70, 720	92.7	38
Magnetic catalyst from palm kernel shell	Waste cooking oil	13:1, 3.66, 65, 120	90.2	42
Jatropha hulls	Jatropha crude oil	18:1, 7.5, 180, 450	95.9	39
Rubber de-oiled cake	Waste cooking oil	12.8:1, 8.18, 63, 60	91.2	43
Cacao shell	Oleic acid	7:1, 5, 45, 1440	94	44
Sodium peroxide/sulfonic acid-functionalized SBA-16	Waste cooking oil	18:1, 10g, 65, 240	93	40
Corncobs and calcined poultry	Neem seed oil	14.76:1, 2.58, 61.9, 72.65	92.89	41
Ce supported activated coconut shell	Chicken fat oil	12:1, 3, 90, 60	93	37

[a]Methanol to oil ratio, catalyst (wt % unless otherwise indicated), temperature (°C), time (min).

synthesis of these catalysts necessitates a high calcination temperature and a longer period, limiting their industrial applicability.

Fuel Characteristics Study. The production of UCOME was validated by GC analysis, performed in an Agilent GC system assembled with an INNOWAX column. As seen in Figure S4, the reaction was successful because the FFAs in the oil were transformed into the appropriate methyl esters.[28] The formed ester of the GC analysis is depicted in Table S4.

The FTIR spectra of the produced UCOME are shown in Figure S5 displays. The UCOME was compared to UCO as displayed in Figure S5a,b. Both the UCO and UCOME showed similar peaks except the peak at 1078.62 and 956 cm^{-1}, which confirms the production of UCOME. FTIR investigations are used in many reports to analyze the formation of biodiesel. Rabelo et al. reported that the component of methyl ester exists in the range of 1800−1700 cm^{-1}. This peak defines the stretching of C═O, signifying esters.[45] Based on Figure S5b the absorption peak that reflected the ester for this research work was observed at 1744.63 cm^{-1}. The main spectrum region that confirms the formation of UCOME is between 1500 and 900 cm^{-1}. The peak at 1462.04 cm^{-1} signifies the ester ($-CH_3$) spectrum. The stretching of O−CH_3 at 1165.51 cm^{-1} is a typical biodiesel peak.[46] In addition, Rafati et al. also obtained a similar ester peak at 1163 cm^{-1}.[47] The peaks found in this research work are 2921.05, 2852.76, 1367.45, 1114.85, 1078.62, and 724.21 cm^{-1}.[48]

The UCOME production is also substantiated from the proton NMR analysis as shown in Figure S6. The presence of methoxy protons and α-CH_2 protons in the ester was confirmed as a result of the singlet peak observed at 3.664 ppm and triplet peak detected at 2.850 ppm. Equation 12 was employed to determine the formation of methyl ester based on the integrals of methylene (A_{CH_2}) and methoxy (A_{Me}) groups, resulting in 98.66% from proton NMR analysis.

$$\text{Conversion } (\%) = \frac{2A_{Me}}{3A_{CH_2}} \times 100 \tag{12}$$

where C denotes the FFA conversion % and factors 2 and 3 determine the proton numbers of the methoxy and methylene groups, respectively.

Fuel Properties of the Synthesized UCOME. The fuel attributes of the derived FAME are evaluated and contrasted with those of ordinary diesel. Table 5 lists the characteristics evaluated by ASTM standards. Low FFA and AN levels in the fuel are a good sign that the fuel will not corrode the metallic engine components. For information on the fluidity and spray properties of the fuel during fuel injection, an estimation of kinematic viscosity (KV) is required. KV is found to be 2.2 mm^2/s. Because the ester had a low moisture content, hydrolysis would be less likely to occur. The fuel has a high fire point of 189 °C and a flash point of 180 °C, implying that it is thermally stable and safe for storage or transportation. The aniline point is comparable to ordinary diesel, indicating that the product has a higher aromatic component. Additionally, the fuel's cetane number is within the suitable range for the standard of diesel. The high calorific value of 40.44 MJ/kg further demonstrates that the fuel is energy-potent. The ester content discovered by the standard (EN14103) for ester characterization was higher than the necessary 96.4%.

Table 5. Analysis of Used Cooking Oil and Used Cooking Oil Methyl Ester Obtained

Parameter	Used cooking oil	Used cooking oil methyl ester	Standards
Acid Value (mg KOH/g)	16.89	0.21	ASTM D974
Free fatty acid (%)	8.49	0.11	
Kinematic viscosity (mm^2/s)	8.57	2.2	ASTM D445
Relative density (25 °C)	0.91	0.815	ASTM D4253
Calorific value (MJ/kg)	36.35	40.44	ASTM D6751
Water content (%)	1.8	0.045	ASTM D3172
Flash point (°C)		180	ASTM 6450
Fire point (°C)		189	ASTM 6450
Aniline point (°C)		49.5	ASTM D611
Cetane Number		51.3	ASTM D613
Ester content (%)		97.2	EN14103

CONCLUSION

This research investigation substantiated the utilization of novel sulfonated *Tamarindus indica* carbon as a catalyst for producing biodiesel from used cooking oil using the RSM. Using SDC catalyst (5 wt %), the esterification of UCO with methanol with 40 wt % concentration gave 98.97% UCOME conversion after 90 min at 60 °C, while esterification of UCO produced a conversion of 98.97%, which is apparently noticed to be more remarkable than the earlier published works at relatively lower reaction temperature. According to the ANOVA results, all of the investigated parameters have a substantial effect on UCOME conversion, except the reaction time, which has a compelling outcome on the reported

https://doi.org/10.1021/acssusresmgt.3c00111
ACS Sustainable Resour. Manage. XXXX, XXX, XXX−XXX

conversion. The experimental confirmation of the projected optimum conditions validates the model's validity once more, and the obtained results are deemed satisfactory when compared to the projected output. The E_a for the esterification reaction was discovered to be 61.012 kJ/mol, and its kinetics suited the first-order reaction well. This indicates that very little energy is needed for the reaction to occur very vigorously. The UCOME was put through GC, FTIR, and ^{1}H NMR analysis to ascertain the structural proportions of the methyl esters formed. The content of ester, as per the European standard 14103, was determined to be greater than the minimal threshold. The biodiesel's characteristics were in line with ASTM requirements. Because of its high fire and flash points, the UCOME was excellent for both storage and transportation. Tests using cetane numbers verified that the fuel has reduced combustion delays than conventional diesel and is of sufficient grade for use as industrial biodiesel. As a result, it can be combined with other fuels or used entirely in place of petro-diesel. The catalyst can also be employed for four successive cycles of reactions. In our laboratories, more efforts are being undertaken to lessen the loss of catalyst function. Sulfonated *Tamarindus indica* carbon created locally is significantly more affordable ($1.054) than activated char acquired from the vendor ($14.6), as per the examination of the expenses concerned with creating the catalyst, which provides a significant pathway for industrialization. The final cost of the prepared catalyst was evaluated to be $3.706/kg. This suggested that the process has the potentiality for commercial application. A cost analysis reveals that the catalyst's production is relatively simple and produces high-quality ester with widespread commercialization potential.

■ ASSOCIATED CONTENT

Supporting Information

The Supporting Information is available free of charge at https://pubs.acs.org/doi/10.1021/acssusresmgt.3c00111.

ANOVA esterification results, fit and model comparison characteristics, process parameter values, graphs of predicted vs actual results, studentized residuals vs predicted, normal regression plot, and residual graph, 3D surface image, plots of X vs time, k vs temperature, and thermodynamic graph of conversion, gas chromatogram and analysis results, FTIR spectrum, ^{1}H NMR spectrum. The results of the investigative parametric runs are assessed and consolidated utilizing ANOVA statistical analyses, as seen in Table S1. Table S1 suggests that all the parameters have influence on the esterification reaction. Additionally, the model shows a significant correlation between actual and hypothetical data, with the R^2 values for hypothetical and actual data as shown in Table S2 (0.9954 and 0.9982, respectively). Table S3 has listed the effect and contribution of individual parameters. Diagnostic graphs are utilized to predict the reliability of predicted and actual conversion (Figure S1). A three-dimensional diagram (Figure S2) was applied to assess the outcome of autonomous parameters on the synthesis of UCOME from used cooking oil. Figure S3 depicts the thermodynamic nature of the performed reaction. Table S4 lists out the presence of different ester in the produced UCOME. The production of UCO to UCOME was validated by Figure S4, i.e., GC analysis. The reaction was successful because the FFAs in the oil were transformed into the appropriate methyl esters. The FTIR spectra of the produced UCOME are shown in Figure S5. The UCOME was compared to UCO as displayed in Figure S5a,b. Both the UCO and UCOME showed similar peaks except the peak at 1078.62 and 956 cm^{-1}, which confirms the production of UCOME. Figure S6 substantiated UCOME production from the proton NMR. The presence of methoxy protons and α-CH_2 protons in the ester was confirmed as a result of the singlet peak observed at 3.664 ppm and triplet peak detected at 2.850 ppm. (PDF)

■ AUTHOR INFORMATION

Corresponding Author

Gopinath Halder − *Chemical Engineering Department, National Institute of Technology Durgapur, Durgapur 713209 West Bengal, India;* orcid.org/0000-0002-9412-0315; Email: ghalder.che@nitdgp.ac.in

Authors

Nabanita Ghosh − *Chemical Engineering Department, National Institute of Technology Durgapur, Durgapur 713209 West Bengal, India*

Rhithuparna D − *Chemical Engineering Department, National Institute of Technology Durgapur, Durgapur 713209 West Bengal, India;* orcid.org/0000-0001-7256-2342

Samuel Lalthazuala Rokhum − *Chemistry Department, National Institute of Technology Silchar, Silchar 788010 Assam, India;* orcid.org/0000-0001-8820-569X

Complete contact information is available at: https://pubs.acs.org/10.1021/acssusresmgt.3c00111

Author Contributions

Nabanita Ghosh: Conceptualization, Methodology, Writing−original draft. **Rhithuparna D**: Formal analysis, Software. **Samuel Lalthazuala Rokhum**: Supervision, Writing−review & editing. **Gopinath Halder**: Supervision, Project administration, Writing−review & editing.

Notes

The authors declare no competing financial interest.

■ ACKNOWLEDGMENTS

The authors are thankful to Department of Chemical Engineering, National Institute of Technology, where the experiments were carried out.

■ REFERENCES

(1) Dawodu, F. A.; Ayodele, O.; Xin, J.; Zhang, S.; Yan, D. Effective Conversion of Non-Edible Oil with High Free Fatty Acid into Biodiesel by Sulphonated Carbon Catalyst. *Appl. Energy* **2014**, *114*, 819−826.

(2) Adewale, P.; Vithanage, L. N.; Christopher, L. Optimization of Enzyme-Catalyzed Biodiesel Production from Crude Tall Oil Using Taguchi Method. *Energy Convers. Manag.* **2017**, *154* (November), 81−91.

(3) Ajala, E. O.; Ajala, M. A.; Okedere, O. B.; Aberuagba, F.; Awoyemi, V. Synthesis of Solid Catalyst from Natural Calcite for Biodiesel Production: Case Study of Palm Kernel Oil in an Optimization Study Using Definitive Screening Design. *Biofuels* **2021**, *12* (6), 703−714.

(4) Olubunmi, B. E.; Karmakar, B.; Aderemi, O. M.; G, A. U.; Auta, M.; Halder, G. Parametric Optimization by Taguchi L9 Approach

towards Biodiesel Production from Restaurant Waste Oil Using Fe-Supported Anthill Catalyst. *J. Environ. Chem. Eng.* **2020**, *8* (5), 104288.
(5) Hosseinzadeh-Bandbafha, H.; Tabatabaei, M.; Aghbashlo, M.; Khanali, M.; Demirbas, A. A Comprehensive Review on the Environmental Impacts of Diesel/Biodiesel Additives. *Energy Convers. Manag.* **2018**, *174* (August), 579−614.
(6) Didar, Z. A Comparative Study of Biodiesel Production from Beef Bone Marrow. *J. Food Biosci. Technol.* **2015**, *5* (2), 61−66.
(7) Vargas, E. M.; Neves, M. C.; Tarelho, L. A. C.; Nunes, M. I. Solid Catalysts Obtained from Wastes for FAME Production Using Mixtures of Refined Palm Oil and Waste Cooking Oils. *Renew. Energy* **2019**, *136*, 873−883.
(8) Al-Tikrity, E. T. B.; Fadhil, A. B.; Ibraheem, K. K. Biodiesel Production from Bitter Almond Oil as New Non-Edible Oil Feedstock. *Energy Sources, Part A Recover. Util. Environ. Eff.* **2017**, *39* (7), 649−656.
(9) Badawy, T.; Mansour, M. S.; Daabo, A. M.; Abdel Aziz, M. M.; Othman, A. A.; Barsoum, F.; Basouni, M.; Hussien, M.; Ghareeb, M.; Hamza, M.; Wang, C.; Wang, Z.; Fadhil, A. B. Selection of Second-Generation Crop for Biodiesel Extraction and Testing Its Impact with Nano Additives on Diesel Engine Performance and Emissions. *Energy* **2021**, *237*, 121605.
(10) Topare, N. S.; Patil, K. D.; Khedkar, S. V. Synthesis of Biodiesel from Waste Cooking Oil and Emission Characteristics of Its Blends. *IOP Conf. Ser. Mater. Sci. Eng.* **2020**, *983* (1), 012015.
(11) Mohadesi, M.; Aghel, B.; Maleki, M.; Ansari, A. The Use of KOH/Clinoptilolite Catalyst in Pilot of Microreactor for Biodiesel Production from Waste Cooking Oil. *Fuel* **2020**, *263* (September), 116659.
(12) Chowdhury, S.; Dhawane, S. H.; Jha, B.; Pal, S.; Sagar, R.; Hossain, A.; Halder, G. Biodiesel Synthesis from Transesterified Madhuca Indica Oil by Waste Egg Shell-Derived Heterogeneous Catalyst: Parametric Optimization by Taguchi Approach. *Biomass Convers. Biorefinery* **2021**, *11* (4), 1171−1181.
(13) Dhawane, S. H.; Bora, A. P.; Kumar, T.; Halder, G. Parametric Optimization of Biodiesel Synthesis from Rubber Seed Oil Using Iron Doped Carbon Catalyst by Taguchi Approach. *Renew. Energy* **2017**, *105*, 616−624.
(14) Altikriti, E. T.; Fadhil, A. B.; Dheyab, M. M. Two-Step Base Catalyzed Transesterification of Chicken Fat: Optimization of Parameters. *Energy Sources, Part A Recover. Util. Environ. Eff.* **2015**, *37* (17), 1861−1866.
(15) Helmi, M.; Tahvildari, K.; Hemmati, A.; Aberoomand azar, P.; Safekordi, A. Phosphomolybdic Acid/Graphene Oxide as Novel Green Catalyst Using for Biodiesel Production from Waste Cooking Oil via Electrolysis Method: Optimization Using with Response Surface Methodology (RSM). *Fuel* **2021**, *287* (October), 119528.
(16) Bora, A. P.; Konda, L. D. N. V. V.; Pasupuleti, S.; Durbha, K. S. Synthesis of MgO/MgSO4 Nanocatalyst by Thiourea-Nitrate Solution Combustion for Biodiesel Production from Waste Cooking Oil. *Renew. Energy* **2022**, *190*, 474−486.
(17) Medina-Valtierra, J.; Sánchez-Olmos, L. A.; Carrasco-Marin, F.; Sánchez-Cárdenas, M. Optimization Models Type Box-Behnken in the Obtaining of Biodiesel from Waste Frying Oil Using a Large-Acidity Carbonaceous Catalyst. *Int. J. Chem. React. Eng.* **2017**, *15* (6), 1−15.
(18) Dhawane, S. H.; Kumar, T.; Halder, G. Parametric Effects and Optimization on Synthesis of Iron (II) Doped Carbonaceous Catalyst for the Production of Biodiesel. *Energy Convers. Manag.* **2016**, *122*, 310−320.
(19) Hajjari, M.; Tabatabaei, M.; Aghbashlo, M.; Ghanavati, H. A Review on the Prospects of Sustainable Biodiesel Production: A Global Scenario with an Emphasis on Waste-Oil Biodiesel Utilization. *Renew. Sustain. Energy Rev.* **2017**, *72* (November 2016), 445−464.
(20) Knothe, G.; Razon, L. F. Biodiesel Fuels. *Prog. Energy Combust. Sci.* **2017**, *58*, 36−59.
(21) Zhou, H.; Wang, Z.; Gao, C.; Sun, Q.; Liu, J.; She, D. Synthesis of Honeycomb Lignin-Based Biochar and Its High-Efficiency Adsorption of Norfloxacin. *Bioresour. Technol.* **2023**, *369* (November 2022), 128402.
(22) Keera, S. T.; El Sabagh, S. M.; Taman, A. R. Castor Oil Biodiesel Production and Optimization. *Egypt. J. Pet.* **2018**, *27* (4), 979−984.
(23) Abdullah, R. F.; Rashid, U.; Ibrahim, M. L.; Hazmi, B.; Alharthi, F. A.; Nehdi, I. A. Bifunctional Nano-Catalyst Produced from Palm Kernel Shell via Hydrothermal-Assisted Carbonization for Biodiesel Production from Waste Cooking Oil. *Renew. Sustain. Energy Rev.* **2021**, *137*, 110638.
(24) Gualberto Zavarize, D.; Braun, H.; Diniz de Oliveira, J. Methanolysis of Low-FFA Waste Cooking Oil with Novel Carbon-Based Heterogeneous Acid Catalyst Derived from Amazon Açaí Berry Seeds. *Renew. Energy* **2021**, *171*, 621−634.
(25) Roslan, N. A.; Zainal Abidin, S.; Abdullah, N.; Osazuwa, O. U.; Abdul Rasid, R.; Yunus, N. M. Esterification Reaction of Free Fatty Acid in Used Cooking Oil Using Sulfonated Hypercrosslinked Exchange Resin as Catalyst. *Chem. Eng. Res. Des.* **2022**, *180*, 414−424.
(26) Jamil, U.; Husain Khoja, A.; Liaquat, R.; Raza Naqvi, S.; Nor Nadyaini Wan Omar, W.; Aishah Saidina Amin, N. Copper and Calcium-Based Metal Organic Framework (MOF) Catalyst for Biodiesel Production from Waste Cooking Oil: A Process Optimization Study. *Energy Convers. Manag.* **2020**, *215* (April), 112934.
(27) Karmakar, B.; Samanta, S.; Halder, G. Delonix Regia Heterogeneous Catalyzed Two-Step Biodiesel Production from Pongamia Pinnata Oil Using Methanol and 2-Propanol. *J. Clean. Prod.* **2020**, *255*, 120313.
(28) Dhawane, S. H.; Karmakar, B.; Ghosh, S.; Halder, G. Parametric Optimisation of Biodiesel Synthesis from Waste Cooking Oil via Taguchi Approach. *J. Environ. Chem. Eng.* **2018**, *6* (4), 3971−3980.
(29) Tang, W.; Gao, M.; Zhang, B.; Wang, X.; Wu, C.; Wang, Q.; Liu, S. Performance and Deactivation Mechanism of a Carbon-Based Solid Acid Catalyst in the Esterification of Soybean Saponin Acid Oil. *J. Environ. Chem. Eng.* **2023**, *11* (3), 109797.
(30) Wang, S.; Xue, Y.; Zhao, X.; Yuan, H. Preparation of a Carbon Microsphere-Based Solid Acid Application to Waste Frying Oil Transesterification. *Diam. Relat. Mater.* **2021**, *116* (November 2020), 108420.
(31) Li, M.; Zheng, Y.; Chen, Y.; Zhu, X. Biodiesel Production from Waste Cooking Oil Using a Heterogeneous Catalyst from Pyrolyzed Rice Husk. *Bioresour. Technol.* **2014**, *154*, 345−348.
(32) Ghosh, N.; Rhithuparna, D.; Khatoon, R.; Lalthazuala, S.; Halder, G. Sulphonic-Acid Functionalized Novel Limonia Acidissima Carbonaceous Catalyst for Biodiesel Synthesis from Millettia Pinnata Oil : Optimization, Kinetics, Thermodynamics and Cost Analysis. *J. Clean. Prod.* **2023**, *394* (November 2022), 136362.
(33) Devasan, R.; Ruatpuia, J. V. L.; Gouda, S. P.; Kodgire, P.; Basumatary, S.; Halder, G.; Rokhum, S. L. Microwave-Assisted Biodiesel Production Using Bio-Waste Catalyst and Process Optimization Using Response Surface Methodology and Kinetic Study. *Sci. Rep.* **2023**, *13* (1), 1−18.
(34) Shuit, S. H.; Tan, S. H. Biodiesel Production via Esterification of Palm Fatty Acid Distillate Using Sulphonated Multi-Walled Carbon Nanotubes as a Solid Acid Catalyst: Process Study, Catalyst Reusability and Kinetic Study. *Bioenergy Res.* **2015**, *8* (2), 605−617.
(35) Putra, M. D.; Irawan, C.; Udiantoro; Ristianingsih, Y.; Nata, I. F. A Cleaner Process for Biodiesel Production from Waste Cooking Oil Using Waste Materials as a Heterogeneous Catalyst and Its Kinetic Study. *J. Clean. Prod.* **2018**, *195*, 1249−1258.
(36) Thushari, I.; Babel, S. Biodiesel Production from Waste Palm Cooking Oil Using Solid Acid Catalyst Derived from Coconut Meal Residue. *Waste and Biomass Valorization* **2020**, *11* (9), 4941−4956.
(37) Shobhana-Gnanaserkhar; Asikin-Mijan, N.; AbdulKareem-Alsultan, G.; Sivasangar-Seenivasagam; Izham, S. M.; Taufiq-Yap, Y. H. Biodiesel Production via Simultaneous Esterification and Trans-esterification of Chicken Fat Oil by Mesoporous Sulfated Ce

https://doi.org/10.1021/acssusresmgt.3c00111
ACS Sustainable Resour. Manage. XXXX, XXX, XXX−XXX

Supported Activated Carbon. *Biomass and Bioenergy* **2020**, *141* (July), 105714.
(38) Thushari, I.; Babel, S. Sustainable Utilization of Waste Palm Oil and Sulfonated Carbon Catalyst Derived from Coconut Meal Residue for Biodiesel Production. *Bioresour. Technol.* **2018**, *248*, 199−203.
(39) Zhang, F.; Tian, X.; Shah, M.; Yang, W. Synthesis of Magnetic Carbonaceous Acids Derived from Hydrolysates of Jatropha Hulls for Catalytic Biodiesel Production. *RSC Adv.* **2017**, *7* (19), 11403−11413.
(40) Su, E. C.; Hsu, J. N.; Lin, Y. C.; Tseng, H. H. Design of a Sodium Peroxide/Sulfonic Acid Functionalized SBA-16 Bi-Functional Catalyst for Improving the Conversion of Waste Cooking Oil to Biodiesel. *Fuel* **2023**, *346* (March), 128274.
(41) Akhabue, C. E.; Osa-Benedict, E. O.; Oyedoh, E. A.; Otoikhian, S. K. Development of a Bio-Based Bifunctional Catalyst for Simultaneous Esterification and Transesterification of Neem Seed Oil: Modeling and Optimization Studies. *Renew. Energy* **2020**, *152*, 724−735.
(42) Quah, R. V.; Tan, Y. H.; Mubarak, N. M.; Kansedo, J.; Khalid, M.; Abdullah, E. C.; Abdullah, M. O. Magnetic Biochar Derived from Waste Palm Kernel Shell for Biodiesel Production via Sulfonation. *Waste Manag.* **2020**, *118*, 626−636.
(43) Malani, R. S.; Shinde, V.; Ayachit, S.; Goyal, A.; Moholkar, V. S. Ultrasound-Assisted Biodiesel Production Using Heterogeneous Base Catalyst and Mixed Non-Edible Oils. *Ultrason. Sonochem.* **2019**, *52* (December 2018), 232−243.
(44) Bureros, G. M. A.; Tanjay, A. A.; Cuizon, D. E. S.; Go, A. W.; Cabatingan, L. K.; Agapay, R. C.; Ju, Y. H. Cacao Shell-Derived Solid Acid Catalyst for Esterification of Oleic Acid with Methanol. *Renew. Energy* **2019**, *138*, 489−501.
(45) Rabelo, S. N.; Oliveira, L. S.; França, A. S. Biodiesel Production From Microwave Irradiated Reactor Using Homogeneous and Heterogeneous Catalysis. *Rev. Eng. Térmica* **2018**, *17* (1), 18.
(46) Jayaprabakar, J.; Dawn, S. S.; Ranjan, A.; Priyadharsini, P.; George, R. J.; Sadaf, S.; Rajha, C. R. Process Optimization for Biodiesel Production from Sheep Skin and Its Performance, Emission and Combustion Characterization in CI Engine. *Energy* **2019**, *174*, 54−68.
(47) Rafati, A.; Tahvildari, K.; Nozari, M. Production of Biodiesel by Electrolysis Method from Waste Cooking Oil Using Heterogeneous MgO-NaOH Nano Catalyst. *Energy Sources, Part A Recover. Util. Environ. Eff.* **2019**, *41* (9), 1062−1074.
(48) Kamaronzaman, M. F. F.; Kahar, H.; Hassan, N.; Hanafi, M. F.; Sapawe, N. Analysis of Biodiesel Product Derived from Waste Cooking Oil Using Fourier Transform Infrared Spectroscopy. *Mater. Today Proc.* **2020**, *31*, 329−332.

https://doi.org/10.1021/acssusresmgt.3c00111
ACS Sustainable Resour. Manage. XXXX, XXX, XXX−XXX